Harnessing Machine Learning Potentials to Understand the Functional Properties of Phase Change Materials

G.C. Sosso*,[1] and M. Bernasconi*,[2]

[1] Department of Chemistry and Centre for Scientific Computing, University of Warwick, Gibbet Hill Road, Coventry CV4 7AL, UK

Email: g.sosso@warwick.ac.uk

[2] Department of Materials Science, University of Milano-Bicocca, Via R. Cozzi 55, I-20125 Milano, Italy

E-mail: marco.bernasconi@unimib.it

The exploitation of phase change materials in diverse technological applications can be greatly aided by a better understanding of the microscopic origin of their functional properties. In the last ten years, simulations based on electronic structure calculations within density functional theory (DFT) have provided useful insights on the properties of materials in this class. Still, large simulation cells and long simulation times beyond the reach of DFT simulations are needed to address several key issues of relevance for the performance of the devices. One way to overcome the limitations of DFT methods is using machine learning techniques to build interatomic potentials for fast molecular dynamics simulations which still retain a quasi-ab initio accuracy. Here, we take stock of what we have learned about the functional properties of the prototypical phase change material GeTe by harnessing such interatomic potentials. Future challenges and applications of the machine learning techniques in the study of phase change materials will be outlined.

Keywords: molecular dynamics, crystal nucleation and growth, machine learning, supercooled liquids, glass aging, phase change materials.

Introduction

The development of novel non-volatile memories (NVMs) is key to further our ability to retain and share the ever-growing amount of data we generate every day (2.5 exabytes in 2013 [1]). Current NVMs based on the Flash technology suffer of a relatively low speed and of a limited endurance. Among the alternative options to Flash technology, phase-change memories (PCMs) [2,3] stand out as one of the

most promising candidates - as testified by the recent Intel/Micron 3D Xpoint technology devised for storage class memories [4].

In PCMs, the information is encoded into two different phases of chalcogenides alloys known as phase change materials [5,6], which can reversibly (up to ~10^5 times) switch between the crystalline and amorphous phases upon Joule heating within few nanoseconds. The two phases have markedly different electrical resistance that are exploited in the memory read out.

Although the $Ge_2Sb_2Te_5$ compound is presently the material of choice for PCM, the quest toward alloys with better performances is very much under way [6,7]. For embedded applications in the automotive industry, for instance, data retention above 100 ^oC is desirable which is not achievable with $Ge_2Sb_2Te_5$. Other applications such as neuromorphic computing [8] or photonic devices [9] would also benefit from a specific tailoring of the functional properties of phase change alloys. To this end, a thorough understanding of the microscopic features of phase change materials is mandatory.

In this respect, atomistic simulations can provide valuable microscopic information difficult to be gained experimentally. First principles (or *ab initio*) electronic structure calculations would be the tool of the trade, and indeed the field has greatly benefited from simulations based on density functional theory (DFT) [6-7,10-12].

Nonetheless, the investigation of many properties of phase change alloys lies well beyond the capabilities of DFT methods: for instance, the crystallization of nanowires (a possible alternative architecture for PCMs) requires simulations of ~10^4 atoms for several nanoseconds, while DFT simulations are typically limited to few hundreds atoms for up to few nanoseconds.

If we were to deal with silicon, we would know what to do: pick an empirical/classical potential of your choice and strike some balance between accuracy (some of which would be lost) and computational efficiency. However, albeit a Tersoff-like parametrization was devised for GeTe [13], phase change materials display a complex interplay between different atomic environments [14], which makes the construction of classical potentials very challenging.

One way to solve this conundrum, where DFT is not fast enough, and classical potentials are not accurate enough, is to harness machine learning (ML) algorithms [15-17] to build interatomic potentials with (quasi) ab initio accuracy *and* a computational efficiency (almost) comparable to that of classical potentials.

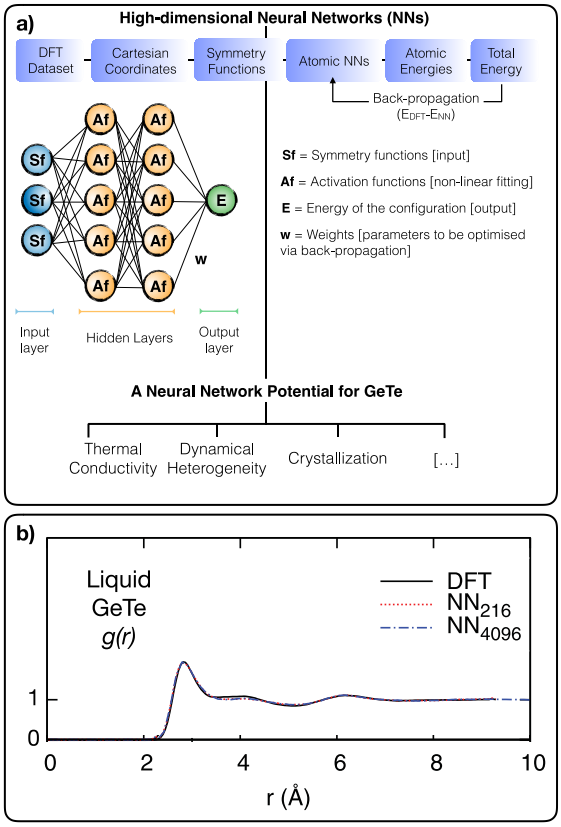

Figure 1. a) Neural networks (NN) can be harnessed to construct a machine learning interatomic potential starting from a dataset of DFT energies of small (100 atoms) configurations. b) Total pair correlation function of liquid GeTe from a NN simulation with 4096 and 216 atoms, compared with DFT results for the smaller cell. Adapted from Ref.[20]. Copyright 2012 American Physical Society.

Machine learning-based interatomic potentials

Machine Learning (ML) is by now a pervasive aspect of technology which is percolating very rapidly into many scientific fields. Materials science is not immune, in that there exists a perception that ML is bound to deliver the next generation of interatomic potentials for atomistic simulations. Actually, in this field ML algorithms are used as a flexible tool to build a potential energy surface by fitting a quite large dataset (10^4-10^5 configurations) of DFT energies and forces of relatively small (10^2 atoms) configurations; two popular approaches in this context are based on Gaussian approximations [18] or neural networks (NNs) [19].

In the NN method of Behler and Parrinello [19] the structure of the system is encoded by means of so-called symmetry functions which describe the local atomic environment of each atom up to a cutoff radius typically encompassing up

to the 3rd coordination shell. As depicted in Figure 1a, the symmetry functions represent the input of a feed-forward NN which consists of a collection of nodes and layers where the inputs are subject to a non-linear transformation (via so-called activation functions) and then linearly combined via a number of "weights" to eventually yield the total energy of a given configuration. The weights are randomly initialized and then refined by backpropagation in order to minimize the mismatch between the energies predicted by the NN and by DFT [19]. Once a sufficiently good fitting is achieved, we can leverage it to obtain the energy of very large models at a low computational cost that scales linearly with the number of atoms. Crucially, forces and stress are readily available from NN potentials, thus enabling fast molecular dynamics (MD) simulations while retaining an accuracy very close to that of the underlying DFT calculations.

In the next sections, we will illustrate how the neural network potential (NNP) for the prototypical phase change compound GeTe that we generated in 2012 [20], has allowed us to address several properties ranging from dynamical heterogeneity and fast crystallization in the liquid phase to the structural relaxations in the glass.

Functional properties of the phase change material GeTe

A neural network potential for GeTe

The NNP for GeTe described in Ref. [20,21] was constructed from the DFT energies of ~30,000 configurations containing from 64 to 216 atoms. The potential was validated against DFT calculations (an example is illustrated in Fig. 1b) and it is capable to describe the bulk phases of GeTe as well as surfaces, nanowires and nanoparticles.

As a first application, the NNP was used to compute the thermal conductivity of the amorphous phase [22] and the thermal boundary resistance at the amorphous-crystal interface [23]. On this topic, we refer the reader to a recent review on the thermal properties of amorphous materials studied by means of ML potentials [24].

Fragility of the supercooled liquid and structural relaxations in the glass

In a PCM device, the crystallization of the amorphous phase is achieved by electrical pulses that bring the material in a supercooled liquid state above the glass transition temperature T_g. One of the key properties of phase change materials is that they tend to be *fragile* liquids [25], which means that their viscosity (η) remains fairly low at high supercooling, only to rise sharply very close to T_g. This feature allows atoms to remain highly mobile at low temperatures (T), where the thermodynamical driving force for crystal nucleation and growth is also high [25]. The NNP allowed us [26] to compute the function η(T) which provided an estimate of the so-called *fragility index* (the slope of η(T) at T_g) which turned out to be in reasonable agreement with later experimental data from ultrafast differential scanning calorimetry [25].

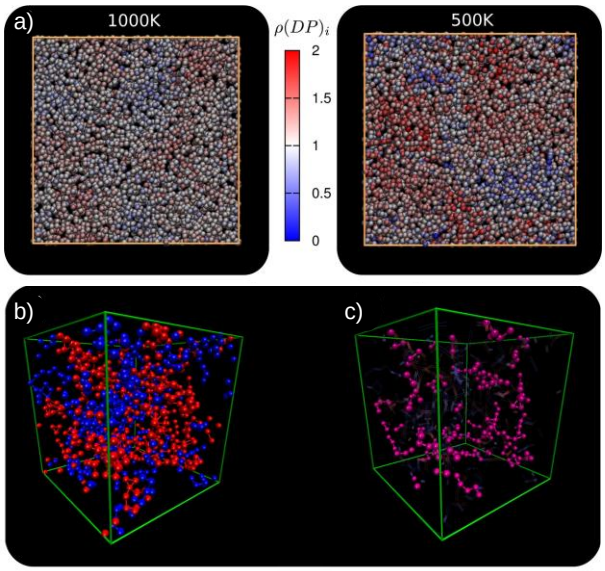

Figure 2. a) Dynamical heterogeneity of liquid GeTe: slow- and fast-moving domains are highlighted in blue and red. b) Spatially localized clusters of slow and fast moving atoms at 500 K. The chains of Ge–Ge bonds in most mobile regions (purple) are highlighted in panel c). Adapted from Ref. [24] - Copyright 2014 American Physical Society.

The atomic mobility at low T is further enhanced by a breakdown of the Stokes-Einstein relation between viscosity and diffusivity that was also predicted by MD simulations [26]. This feature is typical of fragile liquids and it is often ascribed to the emergence of dynamical heterogeneities consisting of spatially separated domains in which atoms move substantially faster or slower than the average. This is illustrated in Figure 2a: close to the melting temperature the distinction between slow (blue) and fast (red) moving regions is minimal; however, as we cool down the system one can clearly notice the emergence of spatially localized domains (see Figure 2b) [27]. These

results have been obtained by the so called isoconfigurational analysis technique, which involves a large number (~100) of MD simulations [27].

Most notably, it turns out that fast-moving regions involve structural heterogeneities in the form of chains of Ge-Ge bonds, depicted in Figure 2c: these chains are not only ultimately responsible for the breakdown of the Stokes-Einstein relation and thus for an enhancement of the atomic mobility at high supercooling which boosts the crystallization speed, but they also play a role in the so-called *resistance drift* – a practical issue for PCMs whereby the resistance of the amorphous phase increases over time due to aging. In fact, by combining NNP and DFT calculations, we have found [28] that Ge-Ge chains are responsible for localized electronic states within the gap of the amorphous phase. Removal of these chains via structural relaxations lead to an energy gain and to a widening of the band gap which can explain the resistance drift (see Ref. [29] for a review).

Moreover, we have recently shown that the presence of Ge-Ge chains provides a rationale for the experimentally measured reduction of the resistance drift in GeTe nanowires [21], whose amorphous structure is characterised, on average, by a lower fraction of Ge-Ge chains compared to the bulk.

Crystal nucleation and growth

From a computational standpoint, the fast crystallization of phase change materials offers the unique opportunity for DFT methods to study crystal nucleation and growth by means of unbiased MD simulations [30]. Indeed, this has been achieved in several works (see Ref. [31] for a review), but the usage of still relatively small models inevitably leads to spurious interactions between the newborn crystalline nuclei and their periodic images, thus affecting both induction times and crystal growth velocities.

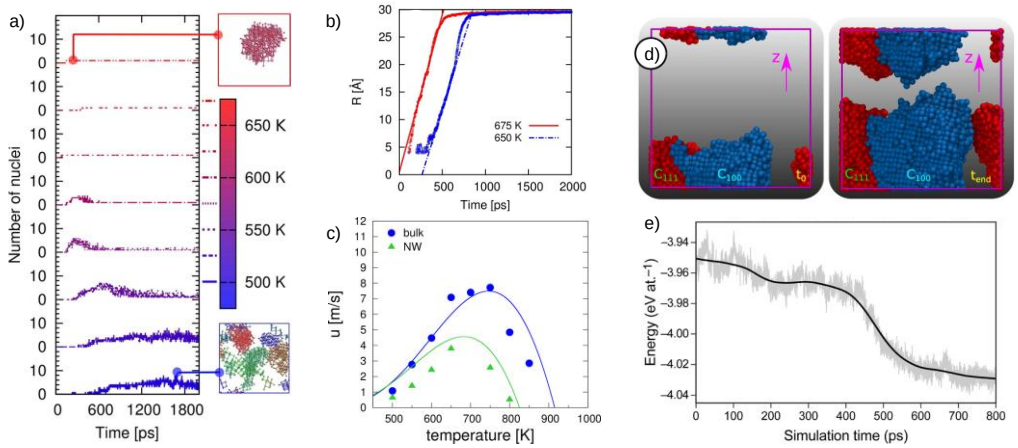

Figure 3. a) Number of crystalline nuclei (> 29 atoms) at different temperatures as a function of time in supercooled liquid GeTe. The number of nuclei first increases and then decreases due to coalescence. The two snapshots show crystalline atoms forming a single nucleus or several nuclei at high or low temperatures. b) The radius R of a crystalline nucleus of GeTe at two temperatures as a function of time. - Reprinted with permission from Ref. [31]. Copyright 2013 American Chemical Society. c) Crystal growth velocity of a GeTe nanowire (green triangles) and at the crystal/liquid interface in the bulk (blue circles). Reprinted with permission from Ref. [21]. Copyright 2017 American Chemical Society. d) C_{111} (red) and C_{100} (blue) crystalline grains in a polycrystalline model of GeTe at the beginning (t_0) and end (t_{end}) of the simulation. Projections along the xz planes are shown. Reprinted with permission from Ref. [31]. Copyright 2015 American Chemical Society. e) Potential energy as a function of time in the simulation of the crystallization of $Ge_2Sb_2Te_5$ with a Gaussian approximation potential. Reprinted with permission from Ref. [35]. Copyright 2018 American Chemical Society.

The advent of NNP was a game changer in this respect, as it allowed us to assess the extent of finite size effects (avoidable by using at least about 1000 atoms) and to investigate crystal nucleation and growth in a wide range of conditions for supercells containing 4000-32000 atoms [32-34]. Some of these findings are summarized in Figure 3: we were able to identify different nucleation regimes at different temperatures (see Figure 3a) and to accurately estimate the crystal growth velocity, extracted from the slope of growth profiles (Figure 3b). Recently, we have compared these growth rates with those obtained for GeTe nanowires [21] (Figure 3c) which enabled the study of the effects of nanostructuring on the crystallization kinetics.

The heterogeneous growth of crystalline GeTe [34] – a scenario of utmost relevance for PCMs - was also addressed by using large models of polycrystalline

GeTe that allowed us to follow the competition between the growth of different grains (Figure 3d).

Moreover, simulations of the crystallization of the most studied ternary compound $Ge_2Sb_2Te_5$ have been performed very recently by means of a ML-based interatomic potential [35] based on Gaussian approximations (the so-called GAP approach [18]): a representative result is reported in Figure 3e.

Conclusions

Although DFT simulations have provided invaluable contributions to the study of phase change materials, there is the need to bring MD simulations closer to the size scale of real PCMs in order to address key issues for the improvement of the devices. ML-based interatomic potentials represent an effective solution, in that they can overcome the limitations of DFT calculations in terms of size and simulation time while offering computational efficiency close to that of classical/empirical potentials.

Here, we have illustrated some of the results we have obtained by means of a NNP for GeTe. The methodologies needed to construct ML potentials are now more accessible than they were in 2012 when the GeTe potential was devised: while a substantial effort is still needed to collect the huge dataset of DFT energies, several promising advances [36,37], including stratified [38] and implanted [39] NN are now available to tackle multi-component alloys [40].

In the field of PCMs, there are open questions that would greatly benefit from large scale simulations of multi-components alloys such as the switching mechanism of Ge-rich alloys for embedded applications [41] and of superlattices/interfacial PCMs [42], just to name a few. For the hotly debated interfacial PCMs [43], DFT simulations have provided a number of different scenarios among which large-scale simulations might ultimately be able to identify the most plausible one. The impact of confinement effects and nanostructuring on the crystallization kinetics is another issue where ML potentials can make a difference. Our previous work on GeTe nanowires is an

example, but much remains to be explored, such as the fascinating possibility of monoatomic PCMs [44] or phase change materials encapsulated in carbon nanotubes [45] or even as isolated nanoparticles [46] .

In conclusion, in light of what the community has achieved in the last few years, we feel that machine learning-based interatomic potentials can truly contribute to the rational design of phase change materials for PCMs and ther applications in the near future.

Acknowledgments

We acknowledge the contributions of several coworkers and in particular of J. Behler, who introduced us to the use of neural network methods.

References

1. *IBM Consumer Products Industry Blog* (2013), (available at https://www.ibm.com/blogs/insights-on-business/consumer-products/2-5-quintillion-bytes-of-data-created-every-day-how-does-cpg-retail-manage-it/).
2. A. Pirovano, A. L. Lacaita, A. Benvenuti, F. Pellizzer, R. Bez, *IEEE Trans. Elect. Dev.* **51**, 452 (2004).
3. A. L. Lacaita, A. Redaelli, *Microelectr. Eng.* **109**, 351 (2013).
4. J. Choe, *TechInsights* http://www.techinsights.com/about-techinsights/overview/blog/intel-3D-xpoint- memory-die-removed-from-intel-optane-pcm (2017).
5. M. Wuttig, N. Yamada, *Nat. Mater.* **6**, 824 (2007).
6. D. Lencer, M. Salinga, M. Wuttig, *Adv. Mater.* **23**, 2030 (2011).
7. F. Rao *et al.*, *Science* **358**, 1423 (2017).
8. G. W. Burr *et al.*, *Adv. Phys. X* **2**, 89 (2016).
9. M. Wuttig, H. Bhaskaran, T. Taubner, *Nat. Photon.* **11**, 465 (2017).
10. S. Caravati, M. Bernasconi, T. D. Kühne, M. Krack, M. Parrinello, *Appl. Phys. Lett.* **91**, 171906 (2007).
11. J. Hegedüs, S. R. Elliott, *Nat. Mater.* **7**, 399 (2008).
12. J. Akola, R. O. Jones, *Phys. Rev. B* **76**, 235201 (2007).
13. F. Zipoli, A. Curioni, *New J. Phys.* **15**, 123006 (2013).
14. V. L Deringer, R. Dobronowski, W. Muttig, *Adv. Func. Mat.* **25**, 6343 (2015).
15. J. Behler, *J. Chem. Phys.* **145**, 170901 (2016).
16. A. P. Bartók *et al.*, *Sci. Adv.* **3**, e1701816 (2017).
17. M. I. Jordan, T. M. Mitchell, *Science* **349**, 255 (2015).
18. A. P. Bartók, G. Csányi, *Int. J. Quantum Chem.* **115**, 1051 (2015).
19. J. Behler, M. Parrinello, *Phys. Rev. Lett.* **98**, 146401 (2007); J. Behler, *Ang. Chem. Int. Ed.* **56**, 12828 (2017).

20. G. C. Sosso, G. Miceli, S. Caravati, J. Behler, M. Bernasconi, *Phys. Rev. B* **85**, 174103 (2012).
21. S. Gabardi *et al.*, *J. Phys. Chem. C* **121**, 23827 (2017).
22. G. C. Sosso, D. Donadio, S. Caravati, J. Behler, M. Bernasconi, *Phys. Rev. B* **86**, 104301 (2012).
23. D. Campi, D. Donadio, G. C. Sosso, J. Behler, M. Bernasconi, *J. Appl. Phys*. **117**, 015304 (2015).
24. G. C. Sosso, V. L. Deringer, S. R. Elliott, G. Csányi, *Mol. Simul.* **44**, 866 (2018).
25. H. Weber, J. Orava, I. Kaban, J. Pries, A. L. Greer, *Phys. Rev. Mater.* **2**, 093405 (2018).
26. G. C. Sosso, J. Behler, M. Bernasconi, *Phys. Status Solidi (b)* **249**, 1880 (2012); *Phys. Status Solidi (a)* **213**, 329 (2016).
27. G. C. Sosso, J. Colombo, J. Behler, E. Del Gado, M. Bernasconi, *J. Phys. Chem. B* **118**, 13621 (2014).
28. S. Gabardi, S. Caravati, G. C. Sosso, J. Behler, M. Bernasconi, *Phys. Rev. B* **92**, 054201 (2015).
29. J.-Y. Raty, *Phys. Status Solidi RRL* **13**, 1800590 (2019).
30. G. C. Sosso *et al.*, *Chem. Rev.* **116**, 7078 (2016).
31. W. Zhang, R. Mazzarello, M. Wuttig, E. Ma, *Nat. Rev. Mater.* **4,** 150 (2019).
32. G. C. Sosso *et al.*, *J. Phys. Chem. Lett.* **4**, 4241 (2013).
33. S. Gabardi *et al.*, *Faraday Discuss.* **213**, 287 (2019).
34. G. C. Sosso, M. Salvalaglio, J. Behler, M. Bernasconi, M. Parrinello, *J. Phys. Chem. C* **119**, 6428 (2015).
35. F. C. Mocanu *et al.*, *J. Phys. Chem. B* **122**, 8998 (2018).
36. H. Chan *et al.*, *J. Phys. Chem. C* **123**, 6941 (2019).
37. L. Zhang, D.-Y. Lin, H. Wang, R. Car, W. E, *Phys. Rev. Mater.* **3**, 023804 (2019).
38. S. Hajinazar, J. Shao, A. N. Kolmogorov, *Phys. Rev. B* **95**, 014114 (2017).
39. B. Onat, E. D. Cubuk, B. D. Malone, E. Kaxiras, *Phys. Rev. B* **97**, 094106 (2018).
40. R. Kobayashi, D. Giofré, T. Junge, M. Ceriotti, W. A. Curtin, *Phys. Rev. Mater.* **1**, 053604 (2017).
41. E. Palumbo, P. Zuliani, M. Borghi, R. Annunziata, *Solid State Elect.* **133**, 38 (2017).
42. R. E. Simpson, P. Fons, A. V. Kolobov, T. Fukaya, M. Krbal, T. Yagi, J. Tominaga, *Nat. Nanotechnol.* ***6***, 501 (2011).
43. M. Boniardi *et al.*, *Phys. Status Solidi (RRL)* **13**, 1800634 (2019).
44. M. Salinga *et al.*, *Nat. Mater.* **17**, 681 (2018).
45. J. M. Wynn *et al.*, *Phys. Rev. Mater.* **1**, 073001 (2017).
46. B. Chen, G. H. ten Brink, G. Palasantzas, B. J. Kooi, *Sci. Rep.* **6**, 39546 (2016).

Figure Captions

Figure 1. a) Neural networks (NN) can be harnessed to construct a machine learning interatomic potential starting from a dataset of DFT energies of small (100 atoms) configurations. b) Total pair correlation function of liquid GeTe from a NN simulation with 4096 and 216 atoms, compared with DFT results for the smaller cell. Adapted from Ref. [20]. Copyright 2012 American Physical Society.

Figure 2. a) Dynamical heterogeneity of liquid GeTe: slow- and fast-moving domains are highlighted in blue and red. b) Spatially localized clusters of slow and fast moving atoms at 500 K. The chains of Ge–Ge bonds in most mobile regions (purple) are highlighted in panel c). Adapted from Ref. [27]- Copyright 2014 American Physical Society.

Figure 3. a) Number of crystalline nuclei (> 29 atoms) at different temperatures as a function of time in supercooled liquid GeTe. The number of nuclei first increases and then decreases due to coalescence. The two snapshots show crystalline atoms forming a single nucleus or several nuclei at high or low temperatures. b) The radius R of a crystalline nucleus of GeTe at two temperatures as a function of time. - Reprinted with permission from Ref. [32]. Copyright 2013 American Chemical Society. c) Crystal growth velocity of a GeTe nanowire (green triangles) and at the crystal/liquid interface in the bulk (blue circles). Reprinted with permission from Ref. [21]. Copyright 2017 American Chemical Society. d) C_{111} (red) and C_{100} (blue) crystalline grains in a polycrystalline model of GeTe at the beginning (t_0) and end (t_{end}) of the simulation. Projections along the xz planes are shown. Reprinted with permission from Ref. [31]. Copyright 2015 American Chemical Society. e) Potential energy as a function of time in the simulation of the crystallization of $Ge_2Sb_2Te_5$ with a Gaussian approximation potential. Reprinted with permission from Ref. [32]. Copyright 2018 American Chemical Society.

Author biographies

Gabriele C. Sosso is an assistant professor of computational physical chemistry at the University of Warwick. He studied materials science at the University of Milano-Bicocca and earned his PhD in Nanostructures and Nanotechnologies from the same institution. He held postdoctoral positions in the research groups of Prof. M. Parrinello and A. Michaelides at ETH Zurich and UCL, respectively. His research focuses on disordered systems and phase transitions, particularly crystal nucleation and growth. Gabriele can be reached via email at g.sosso@warwick.ac.uk.

Marco Bernasconi is full professor of theoretical condensed matter physics and dean of the PhD School in Materials Science and Nanotechnology at the University of Milano-Bicocca, Milano, Italy. He received the PhD in physics from Sissa-Trieste in 1993. After few years at the Max-Planck-Institut in Stuttgart (D), he moved to Milano-Bicocca in 1998. His research focuses on electronic structure calculations and molecular dynamics simulations of materials for applications in microelectronics and photonics. Bernasconi can be reached by email at marco.bernasconi@unimib.it.